Journal of Clinical Biochemistry and Nutrition

Received: December 4, 2024 Accepted: December 7, 2024 Released online: February 6, 2025
DOI: https://doi.org/10.3164/jcbn.24-219

Original Article

Partially hydrolyzed guar gum ingestion suppresses atopic dermatitis-like symptoms through prebiotic effect in mice

So Morishima[1,2], Aya Abe[2], Saki Okamoto[2], Mahendra P. Kapoor[2], Shiho Matsuura[3], Kenji Kuriya[3], Makoto Ozeki[1,2], Masahiro Nishio[3], Hiroto Miura[4], Ryo Inoue[4]*

[1] Laboratory of Food Function, Department of Life Sciences, Graduate School of Bioresources, Mie University, 1577 Kurimamachiya, Tsu, Mie, 514-8507, Japan
[2] Nutrition Division, Taiyo Kagaku Co. Ltd., 1-3 Takaramachi, Yokkaichi, Mie 510-0844, Japan
[3] Laboratory of Nutritional Chemistry, Department of Life Sciences, Graduate School of Bioresources, Mie University, 1577 Kurimamachiya, Tsu, Mie, 514-8507, Japan
[4] Laboratory of Animal Science, Department of Applied Biological Sciences, Faculty of Agriculture, Setsunan University, Nagaotoge-cho 45-1, Hirakata, Osaka 573-0101, Japan

Abstract

Growing knowledge reveals the association between the gut microbiome and skin, rendering the gut microbiome an appealing potential therapeutic target for atopic dermatitis (AD). In this study, we assessed the effect of partially hydrolyzed guar gum (PHGG) on AD-like symptoms induced by topical 1-Chloro-2,4-dinitrobenzene (DNCB) in BALB/c mice. Four weeks of PHGG feeding prevented the loss of epidermal barrier integrity and epithelial hyperplasia in the AD lesion ($p < 0.05$, effect size > 0.80), indicating a reduction in AD-like symptoms. According to the postulated mechanism, PHGG ingestion modulates the gut microbiome resulting in enhanced butyrate production ($p < 0.05$). Butyrate suppresses Th2 function in gut immunity, which is believed to have significance in systemic immune regulation. The lowering of blood Th2 cytokines (IL-4 and IL-10, $p < 0.05$) in the PHGG-fed group confirmed the existence of such a pathway, and butyrate can possibly be considered to have an indirect involvement in the suppression of Th2 immune response in the AD lesions. These findings encourage support for an association between gut microbiome and skin through the immune system, implying that daily PHGG ingestion may be beneficial for suppressing AD symptoms across the gut-immune-skin axis.

Key words: partially hydrolyzed guar gum; atopic dermatitis; gut microbiome; butyrate; immunomodulation

Introduction

Atopic dermatitis (AD) is anticipated to occur in 20-30% of infants, 15-25% of children, and 5-10% of adults, with prevalence expected to increase.[1] It is a type I hypersensitivity with symptoms such as sensitive and dry skin, eczematous lesions and itching sensations, lowering patient's quality of life and incurring a substantial socioeconomic cost.[2] Current remedies include topical steroids, antihistamines, and immunomodulators.[3,4] However, AD involves an array of causes, and existing alternatives to therapy are not effective for every instance of AD. As a result, developing an innovative approach to combat AD remains necessary.

The pathogenesis of AD is complex, and treatment targets are diverse.[5] The association between gut bacteria and skin is referred as the "gut-skin axis" and has lately been recognized as a potential therapeutic target.[6] The gut and harboring bacteria are known to have intricate relationships with the systemic immune system, which implies they play a vital role in the inception and/or progression of systemic medical conditions.[7,8] The relationship between AD and gut bacteria has been debated for a relatively long time, particularly in the context of hygiene hypotheses, and the significance of the gut microbiome in the establishment of immune tolerance has been acknowledged.[9]

Multiple research investigations have demonstrated that prebiotics and probiotics may alleviate AD, with one plausible possibilities involving increased production of short-chain fatty acids (SCFA) in the gut.[10–12] Short-chain fatty acids are organic linear carboxylic acids with six or fewer carbons, the majority of which are produced by gut bacteria during anaerobic fermentation.[13] Butyrate, in particular, is believed to be beneficial for improving AD via the gut-skin axis due to emerging evidence of its anti-inflammatory properties.[14–16] Deficiencies of short-chain fatty acids or short-chain fatty acid-producing bacteria have been identified in young children with AD and their relationship to AD development has been reviewed.[17,18] As a result, increasing SCFA production in the gut could assist with alleviating AD symptoms.

Partially hydrolyzed guar gum (PHGG) is a soluble dietary fiber with prebiotic properties, including the stimulation of SCFA production in the gut.[19–21] It is anticipated to help maintain skin moisture, viscoelasticity and barrier function, in conjunction with the gut-skin axis.[22,23] However, PHGG has never been evaluated for its effect on AD. Therefore, the

present research was undertaken using AD model mice in order to (i) investigate the effect of PHGG on AD improvement and (ii) acquire insights into its probable mechanism associated to the gut-skin axis.

Materials and Methods

Animal

The animal experiments in this work were approved by Mie University's Ethical Experimental Animal Committee (Approval number: 2022-7-MOD) and were carried out in accordance to their guidelines as open-labelled.

Five-week-old female BALB/c mice (Japan SLC, Shizuoka Japan) were randomly separated into three groups (Sham: sham treatment n=5, Control: AD model n=6, and PHGG: AD model plus PHGG feeding n=6) having roughly comparable mean body weights. Sample size was determined in consideration of other relevant studies minimizing the number of animals used in this experiment.[11,24] The animals were kept at a controlled temperature (22 ± 2 °C), relative humidity (60±10%) and light (on/off at 8:00 and 20:00). Every group was housed in one cage. Water and standard chow (AIN-93G, Oriental Bio-Service, Kyoto, Japan) were readily available ad libitum. After a week of acclimatization, AD-like symptoms were elicited using 1-Chloro-2,4-dinitrobenzene (DNCB), as previously reported.[25–27]

Briefly, all mice shaved their dorsal hair using electronic clippers before a day of sensitization and continued to shave every two weeks under isoflurane anesthesia. DNCB solution was prepared by dissolving in fresh acetone and olive oil (3:1) solution at 1% (w/v) for the first sensitization and 0.5% (w/v) for the subsequent challenge. The DNCB challenge entailed applying 100 µl of the solution topically to the dorsal skin and 10µl to the both side of the ear twice per week until the end of the experiment for the Control and PHGG group. Instead of DNCB solution, sham mice received an acetone and olive oil (3:1) solution. After the three weeks of the DNCB challenge, the PHGG group received only modified AIN-93G (5% PHGG instead of 5% cellulose; PHGG is commercially provided as Sunfiber by Taiyo Kagaku Co., Ltd., Mie, Japan) in place of standard AIN-93G. The dose of PHGG was determined to be sufficient to expect a prebiotic effect based on other rodent studies using PHGG.[28,29] The DNCB challenge persisted for a further four weeks for all mice. The brief procedure is summarized in Figure 1.

Dermatitis score and skin trans epidermal water loss (TEWL) were assessed on a regular basis, as described below. Fresh fecal pellets were collected before and four weeks after PHGG feeding and stored at -80 °C for estimating fecal IgA concentration. At the end of the breeding program (three days after final DNCB challenge), all mice were euthanized under isoflurane anesthesia.

The Body and spleen weight were measured using a digital scale. Blood was drawn from the inferior vena cava, and serum was collected using Separapid tube (Kenis, Osaka, Japan). Serum was stored at -80 °C. An electric micrometer was applied to measure the thickness of both ears and the lesion of stripped dorsal skin, which was then fixed with neutral formalin for histological evaluation. The cecal content was collected and stored at -80 °C for analysis of microbiome and organic acids.

Evaluation of dermatitis score and TEWL measurement

The severity of AD symptoms was subjectively assessed using a clinical scale ranging from 0 (no symptoms) to 3 (severe symptoms) for the following items：erythema/hemorrhage, edema, excoriation/erosion, and scaling/dryness.[30] The dermatitis score is defined as the aggregate of those scores (minimum 0, maximum 12). Those evaluations were performed throughout the final four weeks of breeding program (three times per week and once in week seven).

The TEWL of dorsal skin was measured before, two, and four weeks after PHGG feeding using a tewameter (Integral Corporation, Tokyo, Japan) following the manufacturer's protocol. To prevent distress and unexpected injury from restraints, TEWL measurements were performed under isoflurane anesthesia.

Histology

Formalin-fixed skin tissues from the dorsal skin and right ear were embedded in paraffin and sliced into 5 µm sections.

The sections were stained with hematoxylin and eosin (H&E) to assess epithelial structure. A bright-field microscope equipped with a digital camera was employed to capture three and five randomly selected scope fields in the dorsal skin and right ear respectively. The epidermal thickness was measured at three distinct locations per image using the software ImageJ2/Fiji (v2.9.0).

The sections from the same paraffin block were stained with 0.05% toluidine blue solution (pH4.1) for mast cell counting. As previously stated, two or three random scope fields were captured. The mast cell population was counted more than twice in each image, and the area of skin tissue was measured using the ImageJ2/Fiji software to estimate the mast cell number per unit area (cells/mm^2).

Fecal Immunoglobulin A

To dissolve fecal pellets, 10 mg was measured and dissolved 100-fold with 1× Protease Inhibitor Cocktail Set I (Wako, Osaka, Japan). After the 20 minutes of incubation at 4 °C, the

fecal pellet was crushed with a clean pipet chip, vortexed, and incubated for an additional 40 minutes at 4 °C. Centrifuged at 12,000×g and the supernatant was diluted 10-fold with pure water just before the ELISA assay. The IgA Mouse Uncoated ELISA Kit with Plates (Thermo Fisher Scientific, Tokyo, Japan) was used to measure IgA concentration of the samples following the manufacturer's protocol.

Serum IgE and cytokines

Serum IgE was measured using a commercially available kit following the manufacturer's instructions (Mouse IgE ELISA Kit, Bethyl Laboratories, Inc., Texas).

The RayPlex Mouse Inflammation Array 1 Kit (RayBiotech, GA, USA) was used to measure serum levels of G-CSF, IFNγ, IL-1β (IL-1 F2), IL-2, IL-4, IL-6, IL-10, IL-12 p70, IL-17, IL-23 p19, KC (GROα, CXCL1), MCP-1 (CCL2) and TNFα using a BD Accuri C6 flow-cytometer (BD Bioscience, Tokyo, Japan).

Cecal microbiome and organic acids

Cecal DNA was extracted using the QuickGene DNA tissue kit S (KURABO, Osaka, Japan) according to the manufacturer's protocol. DNA fragmentation and library preparation were performed using NEBNext Ultra II FS DNA Library Prep Kit for Illumina and NEBNext Multiplex Oligos for Illumina (Dual Index Primers Set 1) (New England Biolabs, Tokyo, Japan) following the manufacturer's protocol procedure for ≥ 100 ng DNA inputs. AMpure XP beads (Beckman Coulter, Tokyo, Japan) was employed for the size selection and library cleanup process.

The size and concentration of each library were determined using the Bioanalyzer 2100 (Agilent Technologies Japan, Tokyo) with the High Sensitivity DNA kit (Agilent Technologies Japan), following that all libraries were pooled in equimolar amounts. The pooled library was submitted to Rhelixa (Tokyo, Japan) for sequencing data (150-bp paired-end) from the NovaSeq X Plus system (Illumina, San Diego, CA, USA).

Fastp[31] was used to filter low-quality reads with length < 50 base and phred score < Q20. The qualified reads were processed using SqueezeMeta (v1.6.2)[32], an automated metagenomic analysis pipeline. The *de novo* co-assembly was performed using megahit[33]. The R package vegan (v2.6-6.1) was used to conduct diversity analysis. The pairwise-permutational multivariate analysis of variance test was used to compare Bray-Curtis dissimilarity with R package pairwiseAdonis (v0.4.1).

TPM normalized KEGG orthology count data was compared with R package maaslin3 (v0.99.0). KEGG orthologies with $q < 0.05$ and $|\log2 \text{ fold change}| > 1$ were considered

significantly different. KEGG enrichment analysis was conducted with MicrobiomeProfiler (v1.11.1) with significantly different KEGG orthology between Control and PHGG group. KEGG pathways with $q < 0.05$ were considered significantly different between the groups.

The concentrations of cecal organic acids (succinate, lactate, formate, acetate, propionate, butyrate, isobutyrate, valerate, and isovalerate) were determined using ion-exclusion high-performance liquid chromatography, as previously reported.[34]

Statistical analysis

All data are presented as means ± SEM. A one-way analysis of variance (ANOVA) followed by Tukey's HSD test were used for multiple group comparisons. Effect size (Hedge's g) was calculated R package effsize (v0.8.1). Unless otherwise noted, all statistical analyses were performed using R software (v4.2.0). The p-values < 0.05 were considered significant. The effect sizes $g \geq 0.80$ were considered as large.

Results

PHGG reduced the exacerbation of AD-like symptoms induced by continuous DNCB challenge

The mice's body weight increased throughout the experiment, but there was no significant difference between the groups (Fig. 2a). Dermatitis score and TEWL were significantly higher in the DNCB-challenged groups (Control and PHGG) compared with the Sham group, and which was exacerbated by continuous DNCB challenge (Fig. 2b-c). However, dermatitis scores were significantly lower in the PHGG group than in the Control group at one, three and four weeks after PHGG feeding (Fig. 2b, $g = 1.73, 1.73, 1.42$ respectively). TEWL revealed the same pattern as dermatitis scores, and were significantly lower in the PHGG group than in the Control following PHGG feeding (Fig. 2c, $g = 2.06$ and 2.03 at week two and four).

The tissue thickness of the dorsal skin and right ear were significantly greater in the DNCB challenged groups than in the Sham group, whereas there was no significant difference in the left ear (non-DNCB challenged area) across groups (Fig. 2d). Although not statistically significant, the dorsal skin, right ear and tissue thickness difference between right and left ears appeared to be thinner in the PHGG group than in the Control group (Fig. 2d).

The histological evaluation showed that epidermal tissue in the lesions (dorsal skin and right ear) were significantly thicker in the DNCB challenged groups than in the Sham due to cell hyperplasia, although the PHGG group demonstrated significant reduction of

hyperplasia compared to the Control (Fig. 3a-b, g = 3.61 and 2.48 in dorsal skin and right ear). The number of mast cells per unit area in the lesions was significantly increased in the DNCB-treated groups compared to the Sham, whereas it was reduced in the PHGG group compared to Control, albeit non-significant (Fig. 3c-d).

DNCB challenge altered the immune profile and PHGG feeding partially suppressed it

The DNCB challenge significantly increased the weight of the spleen, a key lymphoid organ. However, the increase dropped in the PHGG group compared to the Control group, with a trend to significance ($p < 0.10$, Fig. 4a). The DNCB challenge similarly significantly elevated serum IgE levels, but that were lower in the PHGG group than in the Control (Fig. 4b). Some of serum cytokine concentrations (IL-4 and TNFα) were significantly higher in the Control group compared to the Sham group (Fig. 4d). The PHGG group had significantly lower levels of IL-10 and IL-4 than Control group (Fig. 4d). The serum IFNγ concentration was not shown since the obtained values were outrange of the standard curve.

The amount of fecal IgA, an antibody related to the gut mucosal immunity, was not different between groups before PHGG feeding but significantly increased after four weeks of PHGG feeding compared to other groups (Fig. 4c).

PHGG feeding changed the microbiome to a state rich in butyrate production

The bacterial profile and function of the cecal microbiome were analyzed using whole genome shot-gun sequencing. The analysis excludes the sequence reads from hosts, viruses, eukaryotes or unmapped on any of the reference genomes. The alpha diversity indices of the microbiome revealed no significant variation (Table S1). However, the PHGG group indicated a significantly different microbiome composition compared to the Sham and Control groups in the beta diversity analysis (Fig. 5a).

A comparison of the relative abundance of each bacteria revealed that the abundances of 13 phyla and 135 genera differed significantly between groups (Table S2, Table S3). PHGG feeding was characterized by significant increase in genera such as *Bacteroides*, *Bifidobacterium*, and *Parabacteroides* as well as significant decrease in *Desulfovibrio*, *Dorea*, and *Mucispirillum* among relatively abundant bacteria (>1%, Fig. 5b).

In the cecal organic acid, characteristic cecal bacteria metabolites butyrate and succinate significantly increased by PHGG feeding, while certain organic acids (isobutyrate and formate) were significantly lower in the PHGG group than in the Control group (Fig. 5c, Table S4). We anticipated that the key enzymes involved in PHGG degradation were α-galactosidase and mannan endo-β-1,4-mannosidase and compared the abundances of

bacteria having those genes.[35,36] The bacterial abundances with those genes in the PHGG group were significantly higher than in the Control (Fig. 6a). PHGG feeding significantly enhanced the abundance of ten genera having α-galactosidase gene, including *Acutalibacter*, *Bifidobacterium*, and *Parabacteroides* (Fig. 6b,Table S5). PHGG feeding also significantly enhanced four bacterial genera having mannan endo-β-1,4-mannosidase gene, including *Acutalibacter* and the Lachnospiraceae family (Fig. 6b, Table S6).

The KEGG enrichment analysis (Fig. 6c, TableS7) similarly indicated increased PHGG utilization, with upregulation of the "Starch and sucrose metabolism" and "Fructose and mannose metabolism" pathways in the PHGG group. However, "Galactose metabolism" pathway was downregulated in the PHGG group. Some pathways related to the SCFA production ("Pyruvate metabolism", "Carbon metabolism", "Fatty acid biosynthesis", "Propanoate metabolism") were also upregulated in the PHGG group.

Discussion

The hapten-induced AD animal model used in this study is extensively used in preclinical studies because of its efficiency and reproducibility.[37,38] Although the model utilized in this experiment does not precisely reflect the pathophysiology of AD, the negative spiral of inflammation generated by allergen infiltration and disruption of the epidermal barrier by scratching is well demonstrated, and it is regarded as a reasonable animal model of AD.[37] Since the majority of the Japanese AD population exhibits mild to moderate AD symptoms[39,40], we designed this DNCB challenge approach to assess the significance of PHGG in AD with such severity. As intended, AD-like symptoms in this study was moderate, considering the dermatitis score of other study using DNCB-induced mouse AD model.[27,41,42]

PHGG feeding preserved skin barrier function and minimized skin thickening induced by epidermal hyperplasia, implying that AD-like symptoms were suppressed. One of the mechanisms is thought to be a lowering of Th2 response-associated inflammation, as shown in lower levels of serum Th2 cytokines (IL-4 and IL-10).

The essential function of IL-4 in AD is well documented, and its stimulation has been demonstrated to result in increased Th2 differentiation and IgE class switch in B cells.[43] IgE produced by B cells promotes mast cell degranulation and causes itch-scratching behavior, which leads to epidermal barrier dysfunction and local inflammation, as witnessed in AD.

Therefore, dupilumab (anti-IL-4Rα) received approval by the FDA in 2017 as a first biologic medication for AD therapy[44], highlighting the importance of decreasing IL-4 signaling.[45]

IL-10 has anti-inflammatory activity, although it has been appears to be elevated in the peripheral blood of AD patients.[46,47] IL-4 has been reported to elevate IL-10 expression of Th2 cells, and the low IL-10 levels in the PHGG group in this study might be attributed to IL-4 suppression.[43,48]

Butyrate, one of the gut bacteria-derived metabolites evaluated in this study, is likely to contribute to the suppression of AD-like symptoms. Several studies have revealed that increased gut butyrate and local IL-4 suppression in the skin lesion occur concurrently with the amelioration of AD symptoms.[49–51] Butyrate has been reported to suppress NFκB activation[16], and is expected to contribute to the suppression of inflammation in skin lesions.[24] However, butyrate concentrations in the circulation and peripheral tissues have been reported as quite low (maximum 100 μM in mouse circulation)[52], implying that its direct therapeutic influence in AD lesions is probably constrained. Since gut butyrate concentration is quite higher than peripheral tissues (2-10 mM in this study), and gut immune system performs an essential role in the regulation of the systemic immune system[53], it is likely that the AD improvement by butyrate is derived indirectly via regulation of gut immune system. The increased fecal IgA accompanied by increased cecal butyrate, which is consistent with previous findings[54,55], supports the modulatory effect on the gut immune system by PHGG.

Butyrate has been demonstrated to inhibit Th2 cytokine production[56] and suppress Th2 differentiation via modulating dendritic cell activation in the gut immune system.[52] Therefore, it is suggested that the regulative effect of butyrate on Th2 function in the gut immune system influenced the systemic immune system, resulting in suppression of Th2-mediated inflammation in the skin. Although several studies indicate immuno-modulatory effect of butyrate is accompanied by an elevation in IL-10[49,57,58], IL-10 does not appear to be necessarily involved, as butyric acid have been demonstrated to possess an anti-inflammatory effect even in IL-10$^{-/-}$ mice.[59,60]

Since the exact molecular pathways have not yet been comprehensively elucidated, additional investigation is necessary for understanding how butyrate regulates the immunological response to AD via the gut immune system.

It is anticipated that the increase in PHGG-degrading gut bacteria contributed to the increase in butyrate production. Gut bacteria uses α-glalactosidase and/or mannan endo-ß-1,4-mannosidase to degrade PHGG, yielding monosaccharides and oligosaccharides which can be utilized as carbon sources. As a result, these carbon sources can be used to metabolize SCFA via cross-feeding[61], monosaccharides, and oligosaccharides obtained from PHGG

breakdown likely aided in the production of butyrate. Consequently, an increase in prospective PHGG degraders such as *Acutalibacter*, *Bifidobacterium*, and *Parabacteroides* can be considered significant contributors to enhanced butyrate production. *Parabacteroides*, in particular, is a well-known as fiber degrader, and reported that its increase of abundance enhances SCFA production.[62] KEGG enrichment analysis also demonstrated higher PHGG utilization in the PHGG group, and those gut bacteria appear to prefer mannose as a carbon source over galactose. The "Butanoate metabolism" pathway was not directly enriched in PHGG group, but associated pathways such as "Carbon metabolism" and "Fatty acid biosynthesis" are believed to have contributed to enhanced butyrate generation.

Conclusion

DNCB-induced AD like symptoms were reduced after four weeks of PHGG feeding. In the hypothesized mechanism of this study, enhanced gut butyrate resulting from prebiotic effect of PHGG could be regarded as a key metabolite for AD improvement. Butyrate has already been demonstrated to reduce Th2 differentiation and Th2 cytokine production in the gut immune system, suggesting that it may be implicated in immuno-modulation in AD lesions indirectly. Although specific mechanisms remain to be investigated, the prebiotic effect of PHGG on the immune system, as part of the gut-immune-skin axis, is anticipated to help alleviate AD symptoms. On The other hand, considering the complexity of AD etiology, further research including human clinical trial is needed to elucidate its efficacy on AD.

Author Contributions

SMorishima, AA, MO and RI conceived this experiment; SMorishima, AA, SO, SMatsuura, KK, MN, HM and RI conducted the experiments; SMorishima and RI analyzed data; SMorishima, MPK and RI wrote the manuscript. All authors have read and agreed to the published version of the manuscript.

Funding

This study was partially supported by the Taiyo Kagaku Co., Ltd.

Conflicts of Interest

The author declares no particular conflict of interest. However, referring to a potential conflict of interest, SMorishima, AA, SO, MPK, and MO are employees of Taiyo Kagaku Co., Ltd.; RI and MN received a research support fund from Taiyo Kagaku Co., Ltd.

References

1. Goh MS, Yun JS, Su JC. Management of atopic dermatitis: a narrative review. *Med J Aust* 2022; **216**: 587–593.

2. Bieber T. Atopic dermatitis: an expanding therapeutic pipeline for a complex disease. *Nat Rev Drug Discov* 2022; **21**: 21–40.

3. Frazier W, Bhardwaj N. Atopic Dermatitis: Diagnosis and Treatment. *Am Fam Physician* 2020; **101**: 590–598.

4. Ratchataswan T, Banzon TM, Thyssen JP, Weidinger S, Guttman-Yassky E, Phipatanakul W. Biologics for Treatment of Atopic Dermatitis: Current Status and Future Prospect. *J Allergy Clin Immunol Pract* 2021; **9**: 1053–1065.

5. Gatmaitan JG, Lee JH. Challenges and Future Trends in Atopic Dermatitis. *Int J Mol Sci* 2023; **24**: 11380.

6. Park DH, Kim JW, Park HJ, Hahm DH. Comparative Analysis of the Microbiome across the Gut-Skin Axis in Atopic Dermatitis. *Int J Mol Sci* 2021; **22**: 4228.

7. Wiertsema SP, van Bergenhenegouwen J, Garssen J, Knippels LMJ. The Interplay between the Gut Microbiome and the Immune System in the Context of Infectious Diseases throughout Life and the Role of Nutrition in Optimizing Treatment Strategies. *Nutrients* 2021; **13**: 886.

8. Kim CH. Complex regulatory effects of gut microbial short-chain fatty acids on immune tolerance and autoimmunity. *Cell Mol Immunol* 2023; **20**: 341–350.

9. Inoue R, Nishio A, Fukushima Y, Ushida K. Oral treatment with probiotic Lactobacillus johnsonii NCC533 (La1) for a specific part of the weaning period prevents the development of atopic dermatitis induced after maturation in model mice, NC/Nga. *Br J Dermatol* 2007; **156**: 499–509.

10. Fang Z, Li L, Zhang H, Zhao J, Lu W, Chen W. Gut Microbiota, Probiotics, and Their Interactions in Prevention and Treatment of Atopic Dermatitis: A Review. *Front Immunol* 2021; **12**: 720393.

11. Chen S, Tang L, Nie T, Fang M, Cao X. Fructo-oligofructose ameliorates 2,4-dinitrofluorobenzene-induced atopic dermatitis-like skin lesions and psychiatric comorbidities in mice. *J Sci Food Agric* 2023; **103**: 5004–5018.

12. Rusu E, Enache G, Cursaru R, *et al.* Prebiotics and probiotics in atopic dermatitis. *Exp Ther Med* 2019; **18**: 926–931.

13. He J, Zhang P, Shen L, *et al.* Short-Chain Fatty Acids and Their Association with Signalling Pathways in Inflammation, Glucose and Lipid Metabolism. *Int J Mol Sci* 2020; **21**: 6356.

14. Coppola S, Avagliano C, Sacchi A, *et al.* Potential Clinical Applications of the Postbiotic Butyrate in Human Skin Diseases. *Mol Basel Switz* 2022; **27**: 1849.

15. Chen G, Ran X, Li B, *et al.* Sodium Butyrate Inhibits Inflammation and Maintains Epithelium Barrier Integrity in a TNBS-induced Inflammatory Bowel Disease Mice Model. *eBioMedicine* 2018; **30**: 317–325.

16. Hu C, Zeng D, Huang Y, *et al.* Sodium Butyrate Ameliorates Atopic Dermatitis-Induced Inflammation by Inhibiting HDAC3-Mediated STAT1 and NF-κB Pathway. *Inflammation* 2024; **47**: 989–1001.

17. Barman M, Gio-Batta M, Andrieux L, *et al.* Short-chain fatty acids (SCFA) in infants' plasma and corresponding mother's milk and plasma in relation to subsequent sensitisation and atopic disease. *EBioMedicine* 2024; **101**: 104999.

18. Nylund L, Nermes M, Isolauri E, Salminen S, de Vos WM, Satokari R. Severity of atopic disease inversely correlates with intestinal microbiota diversity and butyrate-producing bacteria. *Allergy* 2015; **70**: 241–244.

19. Slavin JL, Greenberg NA. Partially hydrolyzed guar gum: clinical nutrition uses. *Nutr Burbank Los Angel Cty Calif* 2003; **19**: 549–552.

20. Sakai S, Kamada Y, Takano H, *et al.* Continuous partially hydrolyzed guar gum intake reduces cold-like symptoms: a randomized, placebo-controlled, double-blinded trial in healthy adults. *Eur Rev Med Pharmacol Sci* 2022; **26**: 5154–5163.

21. Matsumiya Y, Kapoor MP, Yamaguchi A, Abe A, Sato N. Synergistic effect of partially hydrolyzed guar gum on Clostridium butyricum in a synbiotic combination for enhanced butyrate production during in-vitro fermentation. *Funct Foods Health Dis* 2024; **14**: 455–469.

22. Kapoor MP, Yamaguchi H, Ishida H, Mizutani Y, Timm D, Abe A. The effects of prebiotic partially hydrolyzed guar gum on skin hydration: A randomized, open-label,

parallel, controlled study in healthy humans. *J Funct Foods* 2023; **103**: 105494.

23. Kapoor MP, Abe A, Morishima S, Nakajima A, Ozeki M, Sato N. Dietary Intervention of Prebiotic Partially Hydrolyzed Guar Gum Improves Skin Viscoelasticity, Stratum Corneum Hydration, and Reduction of Trans-Epidermal Water Loss: A Randomized, Double-Blind, and Placebo-Controlled Clinical Study in Healthy Humans. *J Clin Biochem Nutr* 2025; **76**: 96–115.

24. Trompette A, Pernot J, Perdijk O, Alqahtani RAA, Domingo JS, Camacho-Muñoz D, et al. Gut-derived short-chain fatty acids modulate skin barrier integrity by promoting keratinocyte metabolism and differentiation. *Mucosal Immunol* 2022; **15**: 908–926.

25. Kim JA, Kim SH, Kim IS, *et al.* Galectin-9 Induced by Dietary Prebiotics Regulates Immunomodulation to Reduce Atopic Dermatitis Symptoms in 1-Chloro-2,4-Dinitrobenzene (DNCB)-Treated NC/Nga Mice. *J Microbiol Biotechnol* 2020; **30**: 1343–1354.

26. Yang CC, Hung YL, Ko WC, *et al.* Effect of Neferine on DNCB-Induced Atopic Dermatitis in HaCaT Cells and BALB/c Mice. *Int J Mol Sci* 2021; **22**: 8237.

27. Riedl R, Kühn A, Rietz D, *et al.* Establishment and Characterization of Mild Atopic Dermatitis in the DNCB-Induced Mouse Model. *Int J Mol Sci* 2023; **24**: 12325.

28. Takayama S, Katada K, Takagi T, *et al.* Partially hydrolyzed guar gum attenuates non-alcoholic fatty liver disease in mice through the gut-liver axis. *World J Gastroenterol* 2021; **27**: 2160–2176.

29. Naito Y, Takagi T, Katada K, *et al.* Partially hydrolyzed guar gum down-regulates colonic inflammatory response in dextran sulfate sodium-induced colitis in mice. *J Nutr Biochem* 2006; **17**: 402–409.

30. Takahashi N, Arai I, Honma Y, *et al.* Scratching behavior in spontaneous- or allergic contact-induced dermatitis in NC/Nga mice. *Exp Dermatol* 2005; **14**: 830–837.

31. Chen S, Zhou Y, Chen Y, Gu J. fastp: an ultra-fast all-in-one FASTQ preprocessor. *Bioinforma Oxf Engl* 2018; **34**: i884–i890.

32. Tamames J, Puente-Sánchez F. SqueezeMeta, A Highly Portable, Fully Automatic Metagenomic Analysis Pipeline. *Front Microbiol* 2018; **9**: 3349.

33. Li D, Luo R, Liu CM, *et al.* MEGAHIT v1.0: A fast and scalable metagenome assembler driven by advanced methodologies and community practices. *Methods San Diego Calif* 2016; **102**: 3–11.

34. Morishima S, Abe A, Okamoto S, *et al.* Partially hydrolyzed guar gum suppresses binge alcohol - induced liver fat accumulation via gut environment modulation in mice. *J Gastroenterol Hepatol* 2024; **39**: 2700–2708.

35. Shibuya H, Kobayashi H, Kusakabe I. Galactose Depletion by Mortierella vinacea .ALPHA.-Galactosidase II Increases the Synergistic Interaction between Guar Gum and Xanthan Gum. *Food Sci Technol Res* 1999; **5**: 271–272.

36. Naganagouda K, Salimath PV, Mulimani VH. Purification and characterization of endo-beta-1,4 mannanase from Aspergillus niger gr for application in food processing industry. *J Microbiol Biotechnol* 2009; **19**: 1184–1190.

37. Jin H, He R, Oyoshi M, Geha RS. Animal models of atopic dermatitis. *J Invest Dermatol* 2009; **129**: 31–40.

38. Gilhar A, Reich K, Keren A, Kabashima K, Steinhoff M, Paus R. Mouse models of atopic dermatitis: a critical reappraisal. *Exp Dermatol* 2021; **30**: 319–336.

39. Saeki H, Iizuka H, Mori Y, *et al.* Prevalence of atopic dermatitis in Japanese elementary schoolchildren. *Br J Dermatol* 2005; **152**: 110–114.

40. Saeki H, Oiso N, Honma M, Iizuka H, Kawada A, Tamaki K. Prevalence of atopic dermatitis in Japanese adults and community validation of the U.K. diagnostic criteria. *J Dermatol Sci* 2009; **55**: 140–141.

41. Wang Y, Zhang P, Zhang J, Hong T. Inhibitory Effect of Bisdemethoxycurcumin on DNCB-Induced Atopic Dermatitis in Mice. *Mol Basel Switz* 2022; **28**: 293.

42. Liu T, He Y, Liao Y. Esculentoside A ameliorates DNCB-induced atopic dermatitis by suppressing the ROS-NLRP3 axis via activating the Nrf2 pathway. *Clin Exp Pharmacol Physiol* 2023; **50**: 844–854.

43. Pappa G, Sgouros D, Theodoropoulos K, *et al.* The IL-4/-13 Axis and Its Blocking in the Treatment of Atopic Dermatitis. *J Clin Med* 2022; **11**: 5633.

44. Seegräber M, Srour J, Walter A, Knop M, Wollenberg A. Dupilumab for treatment of

atopic dermatitis. *Expert Rev Clin Pharmacol* 2018; **11**: 467–474.

45. Chiricozzi A, Maurelli M, Peris K, Girolomoni G. Targeting IL-4 for the Treatment of Atopic Dermatitis. *ImmunoTargets Ther* 2020; **9**: 151–156.

46. Liu FT, Goodarzi H, Chen HY. IgE, Mast Cells, and Eosinophils in Atopic Dermatitis. *Clin Rev Allergy Immunol* 2011; **41**: 298–310.

47. Esnault S, Benbernou N, Lavaud F, Shin HC, Potron G, Guenounou M. Differential spontaneous expression of mRNA for IL-4, IL-10, IL-13, IL-2 and interferon-gamma (IFN-gamma) in peripheral blood mononuclear cells (PBMC) from atopic patients. *Clin Exp Immunol* 1996; **103**: 111–118.

48. Schmidt-Weber CB, Alexander SI, Henault LE, James L, Lichtman AH. IL-4 Enhances IL-10 Gene Expression in Murine Th2 Cells in the Absence of TCR Engagement. *J Immunol* 1999; **162**: 238–244.

49. Liu H, Wang J, He T, *et al.* Butyrate: A Double-Edged Sword for Health? *Adv Nutr Bethesda Md* 2018; **9**: 21–29.

50. Kim WK, Jang YJ, Han DH, *et al.* Administration of Lactobacillus fermentum KBL375 Causes Taxonomic and Functional Changes in Gut Microbiota Leading to Improvement of Atopic Dermatitis. *Front Mol Biosci* 2019; **6**: 92.

51. Tang L, Cao X, Chen S, Jiang X, Li D, Chen G. Dietary Galacto-oligosaccharides Ameliorate Atopic Dermatitis-like Skin Inflammation and Behavioral Deficits by Modulating Gut Microbiota–Brain–Skin Axis. *J Agric Food Chem* 2024; **72**: 7954–7968.

52. Yip W, Hughes MR, Li Y, *et al.* Butyrate Shapes Immune Cell Fate and Function in Allergic Asthma. *Front Immunol* 2021; **12**: 628453.

53. Maynard CL, Elson CO, Hatton RD, Weaver CT. Reciprocal interactions of the intestinal microbiota and immune system. *Nature* 2012; **489**: 231–241.

54. Hung TV, Suzuki T. Dietary Fermentable Fibers Attenuate Chronic Kidney Disease in Mice by Protecting the Intestinal Barrier. *J Nutr* 2018; **148**: 552–561.

55. Matsumoto K, Sawano H, Otsubo M, Yui A. Comparison of the Effects of 3 Forms of Soluble Dietary Fiber on the Production of IgA in BALB/cAJcl and BALB/cAJcl-

nu/nu Mice. *J Nutr* 2023; **153**: 1618–1626.

56. Paparo L, Nocerino R, Ciaglia E, *et al.* Butyrate as a bioactive human milk protective component against food allergy. *Allergy* 2021; **76**: 1398–1415.

57. Föh B, Buhre JS, Lunding HB, *et al.* Microbial metabolite butyrate promotes induction of IL-10+IgM+ plasma cells. *PloS One* 2022; **17**: e0266071.

58. Kim DS, Woo JS, Min HK, *et al.* Short-chain fatty acid butyrate induces IL-10-producing B cells by regulating circadian-clock-related genes to ameliorate Sjögren's syndrome. *J Autoimmun* 2021; **119**: 102611.

59. Wang J, Cui M, Sun F, *et al.* HDAC inhibitor sodium butyrate prevents allergic rhinitis and alters lncRNA and mRNA expression profiles in the nasal mucosa of mice. *Int J Mol Med* 2020; **45**: 1150–1162.

60. Lee C, Kim BG, Kim JH, Chun J, Im JP, Kim JS. Sodium butyrate inhibits the NF-kappa B signaling pathway and histone deacetylation, and attenuates experimental colitis in an IL-10 independent manner. *Int Immunopharmacol* 2017; **51**: 47–56.

61. Koh A, De Vadder F, Kovatcheva-Datchary P, Bäckhed F. From Dietary Fiber to Host Physiology: Short-Chain Fatty Acids as Key Bacterial Metabolites. *Cell* 2016; **165**: 1332–1345.

62. Whisner CM, Martin BR, Nakatsu CH, *et al.* Soluble Corn Fiber Increases Calcium Absorption Associated with Shifts in the Gut Microbiome: A Randomized Dose-Response Trial in Free-Living Pubertal Females. *J Nutr* 2016; **146**: 1298–1306.

Supplementary Materials

Table S1: Alpha diversity indices of cecal microbiome; Table S2: Bacterial relative abundance (%) that significantly different between groups at phylum level; Table S3: Bacterial relative abundance (%) that significantly different between groups at genus level; Table S4: Cecal organic acids; Table S5: Bacteria with α-glucosidase gene (%) that significantly different between groups at genus level; Table S6: Bacteria with mannan endo-β-1,4-mannosidase gene (%) that significantly different between groups at genus level; Table S7: Enriched KEGG pathways in microbiome of PHGG group.

Figure Legends

Figure 1. Brief procedure of animal experiment.

Figure 2. Features of PHGG feeding on the DNCB induced AD-like symptoms. Sham (n=5), Control (AD model, n=6), PHGG (AD model + PHGG feeding, n=6). (a) Body weights throughout the experimental period. (b) Dermatitis scores or (c) TEWL values after the PHGG feeding. (d) Tissue thicknesses of the final day of experimental period. Ear (Right-Left) means the difference of tissue thickness between right ear (lesion) and left ear (non-lesion). The significance of the value was determined by Tukey's HSD after a one-way ANOVA and indicated by (b-c) different letters or (d) *$p<0.05$.

Figure 3. PHGG feeding prevented skin epithelial hyperplasia related to DNCB induced AD-like symptoms. Sham (n=5), Control (AD model, n=6), PHGG (AD model + PHGG feeding, n=6). (a) Representative H&E stained tissue section (200×) and (b) measured epidermal thickness. (c) Representative toluidine blue stained tissue section (400×) and (d) counted mast cell number per unit area. The significance of the value was determined by Tukey's HSD after a one-way ANOVA (*$p<0.05$).

Figure 4. Immunological parameters were altered by both of DNCB challenge and PHGG feeding. Sham (n=5), Control (AD model, n=6), PHGG (AD model + PHGG feeding, n=6). (a) Percentage of spleen weight to body weight. (b) Serum IgE concentration. (c) Amount of fecal IgA before and after PHGG feeding. (d) Serum cytokine concentrations (KC : CXCL1). The significance of the value was determined by Tukey's HSD after a one-way ANOVA (*$p<0.05$).

Figure 5. Cecal bacteria composition and its organic acid production were affected by PHGG

feeding. Sham (n=5), Control (AD model, n=6), PHGG (AD model + PHGG feeding, n=6). (a) Principal coordination analysis (PCoA) plot based on Bray-Curtis dissimilarity. The composition was significantly different in the PHGG group compared to the Sham and Control ($p<0.05$, pairwise-PERMANOVA). (b) Bacterial relative abundance that significantly different between groups at genus level. Bacteria were displayed if the genus could be identified and the relative abundance was greater than 1%. (c) Cecal organic acid concentrations. Major SCFA (Acetate, Propionate and Butyrate) and organic acids with significant difference were displayed. (b-e) The significance of the value was determined by Tukey's HSD after a one-way ANOVA (*$p<0.05$) unless otherwise specified.

Figure 6. The function of cecal microbiome was shifted by PHGG feeding to the state high in PHGG degradation and SCFA production. Sham (n=5), Control (AD model, n=6), PHGG (AD model + PHGG feeding, n=6). (a) Relative abundance of total bacteria with α-glucosidase (EC 3.2.1.22) or mannan endo-β-1,4-mannosidase (EC 3.2.1.78) gene. (b) Bacterial genus with α-glucosidase or mannan endo-β-1,4-mannosidase gene that significantly increased with PHGG feeding. (a-b) The significance of the value was determined by Tukey's HSD after a one-way ANOVA (*$p<0.05$) unless otherwise specified. (c) KEGG pathway enrichment analysis of gut microbiome. KEGG orthology of gut microbiome was compared between Control vs PHGG groups. Count is the number of KEGG orthology enriched in the pathway. Regulation (Up/Down) was displayed as the characteristics of PHGG group compared to the Control group. Pathways with significant difference ($q<0.05$) are displayed but those having both Up and Down regulated genes together were excluded.

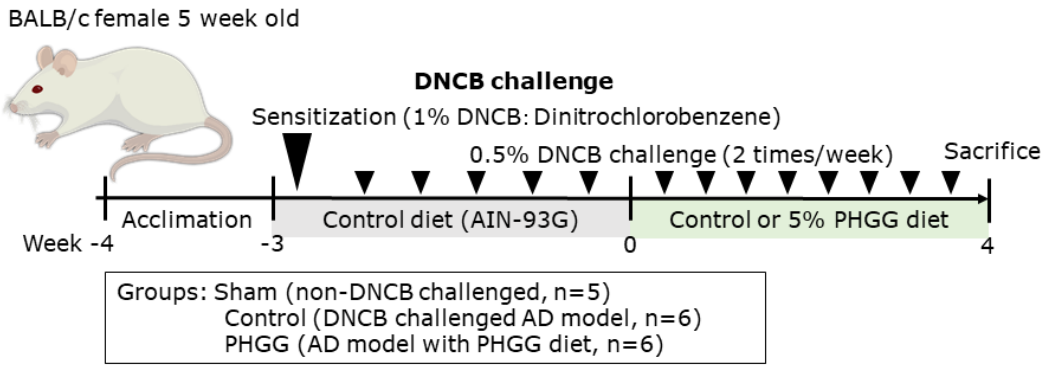

Figure 1. Brief procedure of animal experiment.

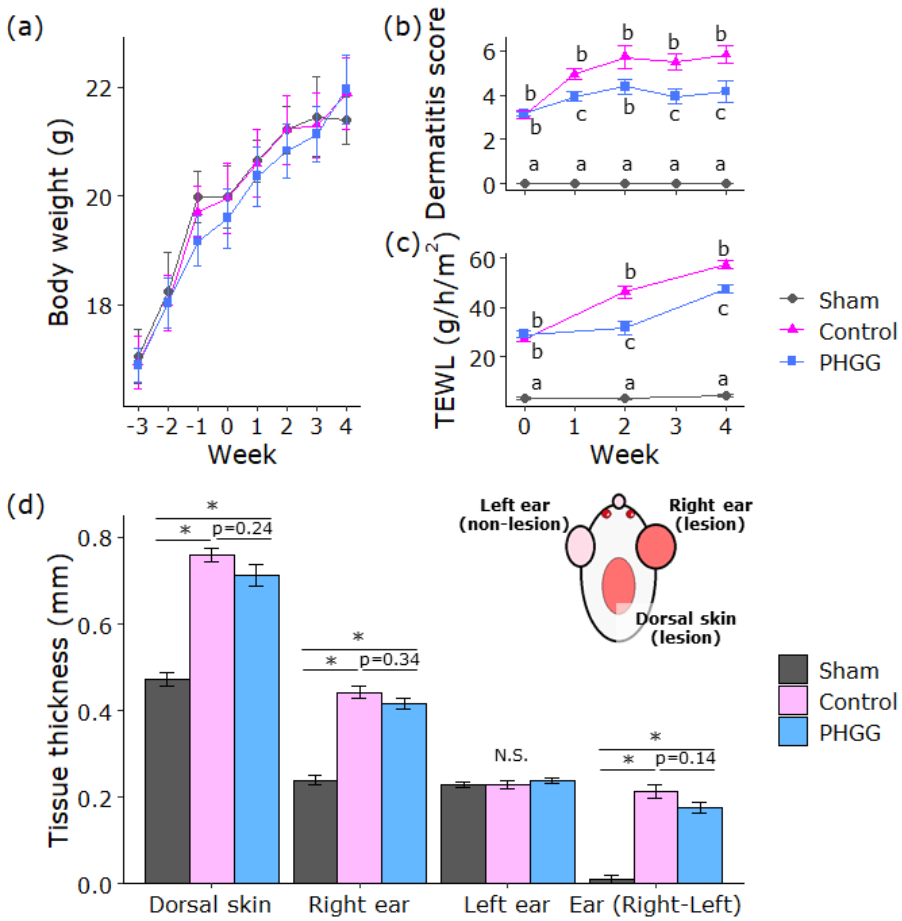

Figure 2. Features of PHGG feeding on the DNCB induced AD-like symptoms. Sham (n=5), Control (AD model, n=6), PHGG (AD model + PHGG feeding, n=6). (a) Body weights throughout the experimental period. (b) Dermatitis scores or (c) TEWL values after the PHGG feeding. (d) Tissue thicknesses of the final day of experimental period. Ear (Right-Left) means the difference of tissue thickness between right ear (lesion) and left ear (non-lesion). The significance of the value was determined by Tukey's HSD after a one-way ANOVA and indicated by (b-c) different letters or (d) *p<0.05.

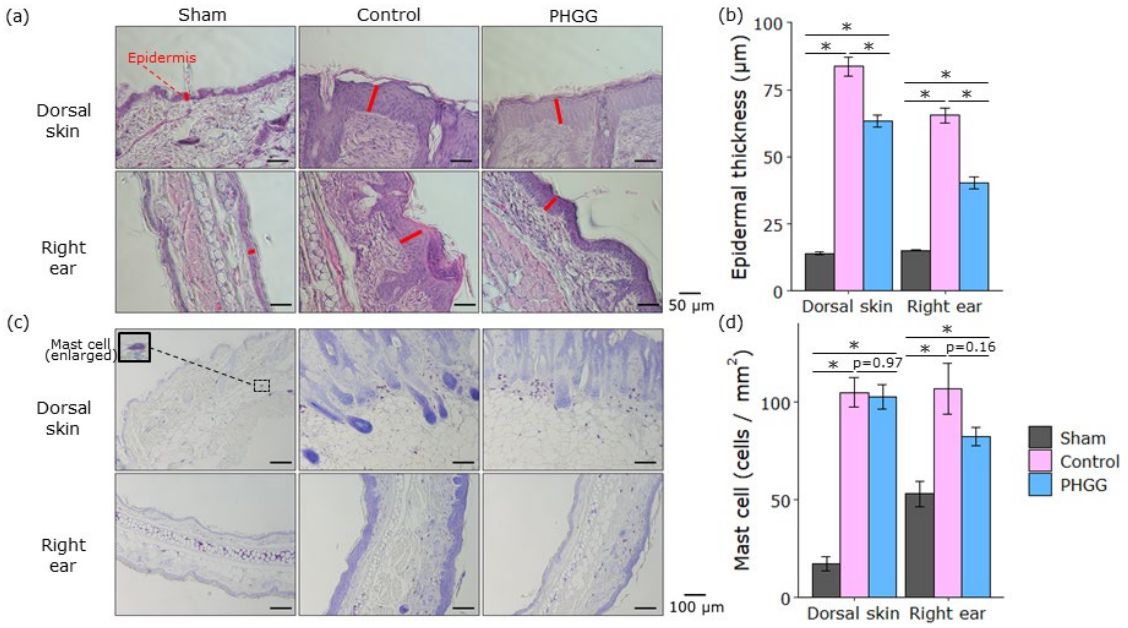

Figure 3. PHGG feeding prevented skin epithelial hyperplasia related to DNCB induced AD-like symptoms. Sham (n=5), Control (AD model, n=6), PHGG (AD model + PHGG feeding, n=6). (a) Representative H&E stained tissue section (200×) and (b) measured epidermal thickness. (c) Representative toluidine blue stained tissue section (400×) and (d) counted mast cell number per unit area. The significance of the value was determined by Tukey's HSD after a one-way ANOVA (*$p<0.05$).

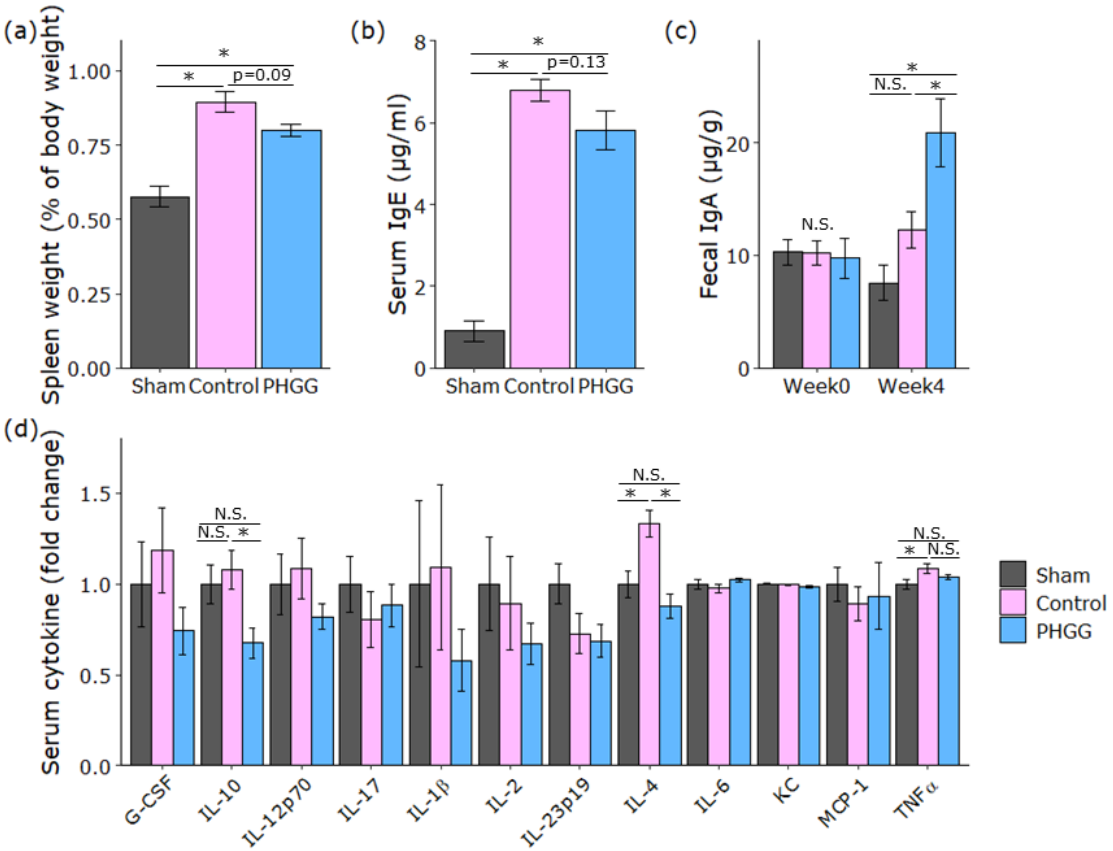

Figure 4. Immunological parameters were altered by both of DNCB challenge and PHGG feeding. Sham (n=5), Control (AD model, n=6), PHGG (AD model + PHGG feeding, n=6). (a) Percentage of spleen weight to body weight. (b) Serum IgE concentration. (c) Amount of fecal IgA before and after PHGG feeding. (d) Serum cytokine concentrations (KC : CXCL1). The significance of the value was determined by Tukey's HSD after a one-way ANOVA (*p<0.05).

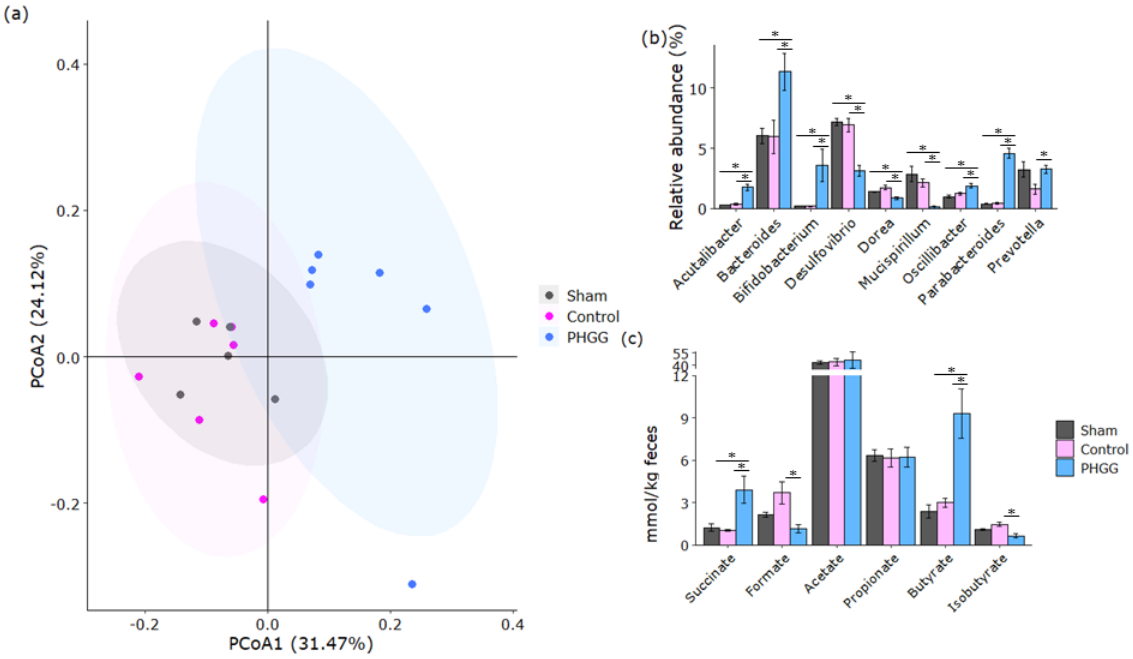

Figure 5. Cecal bacteria composition and its organic acid production were affected by PHGG feeding. Sham (n=5), Control (AD model, n=6), PHGG (AD model + PHGG feeding, n=6). (a) Principal coordination analysis (PCoA) plot based on Bray-Curtis dissimilarity. The composition was significantly different in the PHGG group compared to the Sham and Control ($p<0.05$, pairwise-PERMANOVA). (b) Bacterial relative abundance that significantly different between groups at genus level. Bacteria were displayed if the genus could be identified and the relative abundance was greater than 1%. (c) Cecal organic acid concentrations. Major SCFA (Acetate, Propionate and Butyrate) and organic acids with significant difference were displayed. (b-e) The significance of the value was determined by Tukey's HSD after a one-way ANOVA (*$p<0.05$) unless otherwise specified.

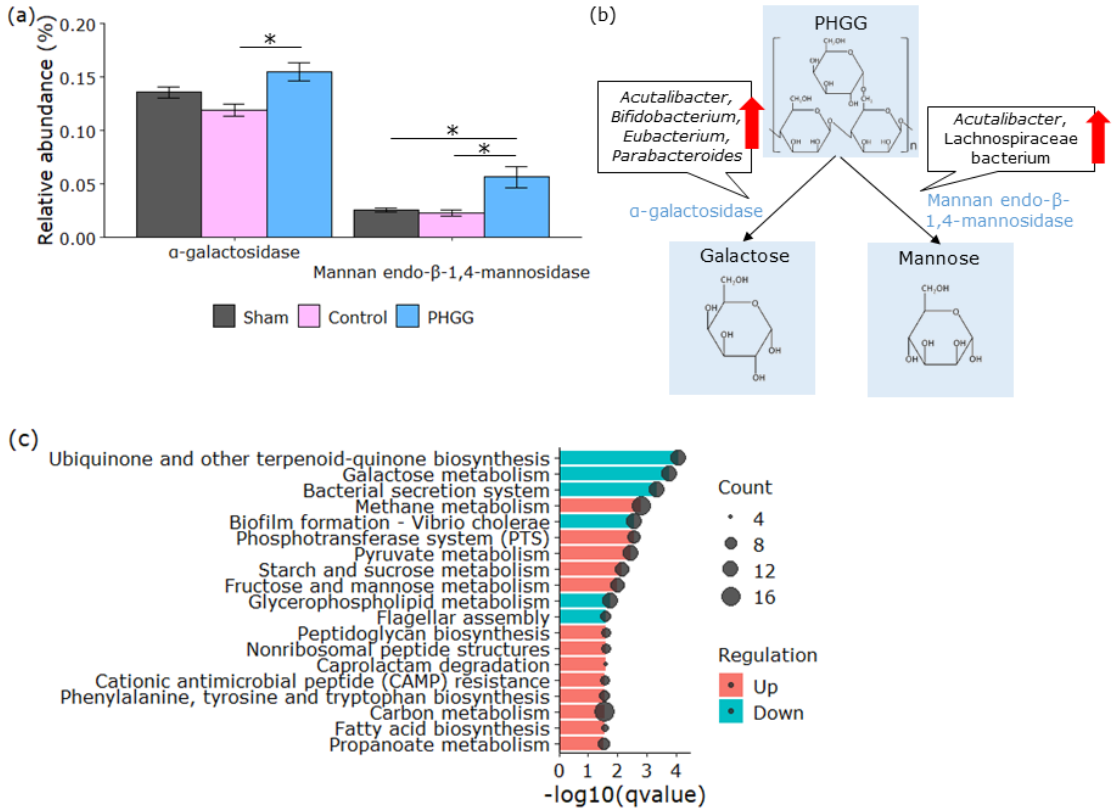

Figure 6. The function of cecal microbiome was shifted by PHGG feeding to the state high in PHGG degradation and SCFA production. Sham (n=5), Control (AD model, n=6), PHGG (AD model + PHGG feeding, n=6). (a) Relative abundance of total bacteria with α-glucosidase (EC 3.2.1.22) or mannan endo-β-1,4-mannosidase (EC 3.2.1.78) gene. (b) Bacterial genus with α-glucosidase or mannan endo-β-1,4-mannosidase gene that significantly increased with PHGG feeding. (a-b) The significance of the value was determined by Tukey's HSD after a one-way ANOVA (*$p<0.05$) unless otherwise specified. (c) KEGG pathway enrichment analysis of gut microbiome. KEGG orthology of gut microbiome was compared between Control vs PHGG groups. Count is the number of KEGG orthology enriched in the pathway. Regulation (Up/Down) was displayed as the characteristics of PHGG group compared to the Control group. Pathways with significant difference ($q<0.05$) are displayed but those having both Up and Down regulated genes together were excluded.

Table S1. Alpha diversity indices of cecal microbiome

Index	Sham	Control	PHGG	One-way ANOVA p-value
Chao1	221.6±2.3	219.2±1.3	214.8±2.3	0.086
Shannon	3.02±0.02	2.93±0.05	2.90±0.05	0.152

Table S2. Bacterial relative abundance (%) that significantly different between groups at phylum level

Phylum	Sham	Control	PHGG	One-way ANOVA p-value	Tukey HSD p-value		
					Shaml vs Control	Control vs PHGG	Sham vs PHGG
Actinobacteria	0.258±0.022	0.235±0.034	4.026±1.428	0.011	>0.999	0.019	0.026
bacterium 0.1xD8-71 (no phylum in NCBI)	0.00014±0.00003	0.00035±0.00006	0.00001±0.00001	<0.001	0.004	<0.001	0.067
bacterium 1XD21-13 (no phylum in NCBI)	0.00136±0.00019	0.00193±0.00012	0.00536±0.00116	0.003	0.852	0.010	0.005
bacterium 1xD42-67 (no phylum in NCBI)	0.022±0.002	0.030±0.001	0.020±0.003	0.022	0.109	0.021	0.739
bacterium 1XD42-76 (no phylum in NCBI)	0.00039±0.00005	0.00051±0.00009	0.00010±0.00005	0.002	0.446	0.002	0.026
bacterium 1xD42-87 (no phylum in NCBI)	0.00107±0.00010	0.00184±0.00040	0.00019±0.00010	0.001	0.132	0.001	0.082
bacterium 1xD8-48 (no phylum in NCBI)	0.00102±0.00011	0.00230±0.00035	0.00127±0.00027	0.013	0.016	0.043	0.807
bacterium c-19 (no phylum in NCBI)	0.00040±0.00006	0.00034±0.00009	0.00174±0.00038	0.001	0.985	0.002	0.005
bacterium D16-50 (no phylum in NCBI)	0.00404±0.00069	0.00297±0.00020	0.00239±0.00029	0.044	0.205	0.567	0.036
Candidatus Saccharibacteria	0.01560±0.00479	0.00016±0.00006	0.00748±0.00295	0.011	0.008	0.216	0.184
Candidatus Sumerlaeota	0.00001±0.00001	0.00003±0.00001	ND	0.008	0.144	0.006	0.307
Deferribacteres	2.921±0.666	2.195±0.345	0.124±0.108	0.001	0.443	0.006	0.001
Proteobacteria	7.762±0.316	7.510±0.593	3.762±0.495	<0.001	0.935	<0.001	<0.001

ND = Not detected

Table S3. Bacterial relative abundance (%) that significantly different between groups at genus level

Genus	Sham	Control	PHGG	One-way ANOVA p-value	Tukey HSD p-value Sham vs Control	Control vs PHGG	Sham vs PHGG
Acetatifactor	0.04477±0.00349	0.0486±0.00359	0.01802±0.00162	<0.001	0.656	<0.001	<0.001
Acetobacter	0.000042±0.000019	ND	0.000003±0.000003	0.022	0.029	0.966	0.046
Acutalibacter	0.2887±0.03173	0.35114±0.05192	1.74833±0.24595	<0.001	0.958	<0.001	<0.001
Alistipes	0.89548±0.08068	0.53789±0.11787	0.03033±0.00204	<0.001	0.025	0.001	<0.001
Alkaliphilus	0.00001±0.00001	0.00004±0.00001	ND	0.019	0.163	0.015	0.504
Alphaproteobacteria bacterium (no genus in NCBI)	0.002193±0.00101	0.000012±0.000004	0.000008±0.000003	0.015	0.025	>0.999	0.025
Anaerobium	0.000017±0.000005	0.001027±0.000101	0.00001±0.000004	<0.001	<0.001	<0.001	0.996
Anaerocaecibacter	0.0607±0.00816	0.07029±0.01861	0.00457±0.00216	0.003	0.851	0.004	0.017
Anaeromassilibacillus	0.00311±0.00043	0.00394±0.00053	0.00609±0.00109	0.045	0.747	0.146	0.047
Anaerostipes	ND	0.000001±0.000001	0.000066±0.000022	0.005	0.998	0.009	0.011
bacterium 0.1xD8-71 (no genus in NCBI)	0.00014±0.00003	0.00034±0.00006	0.00001±0.00001	<0.001	0.004	<0.001	0.07
bacterium 1XD21-13 (no genus in NCBI)	0.00133±0.00018	0.00188±0.00012	0.00521±0.00113	0.003	0.852	0.011	0.005
bacterium 1xD42-67 (no genus in NCBI)	0.02181±0.00241	0.02908±0.00146	0.01912±0.003	0.024	0.122	0.022	0.718
bacterium 1XD42-76 (no genus in NCBI)	0.00038±0.00005	0.0005±0.00009	0.0001±0.00004	0.002	0.45	0.002	0.027
bacterium 1xD42-87 (no genus in NCBI)	0.00104±0.0001	0.0018±0.0004	0.00019±0.0001	0.002	0.137	0.001	0.086
bacterium 1xD8-48 (no genus in NCBI)	0.001±0.0001	0.00224±0.00034	0.00123±0.00027	0.013	0.018	0.041	0.834
bacterium c-19 (no genus in NCBI)	0.00039±0.00006	0.00034±0.00009	0.00168±0.00038	0.002	0.985	0.003	0.006
bacterium D16-50 (no genus in NCBI)	0.00395±0.00067	0.00291±0.0002	0.00229±0.00029	0.039	0.207	0.525	0.032
Bacteroidaceae bacterium (no genus in NCBI)	0.62325±0.08322	0.39596±0.08585	0.00746±0.00093	<0.001	0.083	0.002	<0.001
Bacteroidales bacterium (no genus in NCBI)	0.03574±0.0061	0.0395±0.00647	0.00169±0.001	<0.001	0.865	<0.001	0.001
Bacteroides	6.02683±0.63307	5.95094±1.4034	11.33966±1.52493	0.016	0.999	0.025	0.035
Barnesiella	0.00044±0.00004	0.00031±0.00007	0.00098±0.00014	0.001	0.621	0.001	0.007
Bifidobacterium	0.22057±0.01654	0.20557±0.03298	3.58543±1.35888	0.017	>0.999	0.027	0.036
Butyricicoccus	0.01828±0.00251	0.02682±0.00286	0.0125±0.00275	0.007	0.114	0.005	0.339
Butyricimonas	0.05222±0.00588	0.05042±0.01056	0.01781±0.00466	0.01	0.986	0.021	0.02
Candidatus Coproplasma	0.00003±0.00001	ND	ND	0.001	0.002	>0.999	0.002
ındidatus Saccharibacteria bacterium (no genus in NCI	0.00089±0.00029	0.00001±0.00001	0.00062±0.00023	0.023	0.023	0.105	0.633
Clostridium	0.07696±0.0222	0.00521±0.00034	0.00509±0.00041	0.001	0.001	>0.999	0.001
Colidextribacter	0.02261±0.0022	0.03677±0.00119	0.00779±0.00065	<0.001	<0.001	<0.001	<0.001
Collinsella	0.00007±0.00002	0.00005±0.00001	0.00025±0.00003	<0.001	0.818	<0.001	<0.001
Coprococcus	0.00165±0.00018	0.00173±0.0002	0.00056±0.00008	<0.001	0.927	<0.001	0.001
Desulfovibrio	7.1773±0.29704	6.93874±0.56711	3.13338±0.46383	<0.001	0.935	<0.001	<0.001
Desulfovibrionaceae bacterium (no genus in NCBI)	0.00171±0.00043	0.00113±0.00017	0.00056±0.00003	0.018	0.256	0.233	0.014
Dorea	1.37282±0.06396	1.74012±0.17988	0.87318±0.10151	0.001	0.163	0.001	0.047
Edwardsiella	0.00015±0.00004	0.00009±0.00002	0.00005±0.00001	0.043	0.223	0.526	0.035
Eggerthella	0.000019±0.000009	0.000007±0.000002	0.000232±0.000044	<0.001	0.947	<0.001	<0.001
Eggerthellaceae bacterium (no genus in NCBI)	0.00018±0.00004	0.0001±0.00002	0.00307±0.0004	<0.001	0.971	<0.001	<0.001
Emergencia	0.00012±0.00003	0.00007±0.00002	0.00041±0.00011	0.006	0.887	0.008	0.026
Enterocloster	0.00233±0.00029	0.00357±0.00022	0.00115±0.00021	<0.001	0.007	<0.001	0.01
Enterorhabdus	0.00165±0.00024	0.00122±0.00008	0.02655±0.00357	<0.001	0.99	<0.001	<0.001
Erysipelotrichaceae bacterium (no genus in NCBI)	ND	ND	0.00004±0.00002	0.02	>0.999	0.033	0.042
Evtepia	0.00048±0.00004	0.00059±0.00003	0.00159±0.00011	<0.001	0.578	<0.001	<0.001
Faecalibacterium	0.000038±0.00001	0.000276±0.000015	0.000008±0.000002	<0.001	<0.001	<0.001	0.155
Faecalibaculum	0.19259±0.03916	0.13656±0.02377	0.80194±0.20971	0.004	0.953	0.006	0.016
Faecalicatena	0.000007±0.000005	0.000009±0.000001	0.00009±0.000028	0.007	0.998	0.013	0.015
Feifania	0.000036±0.000009	0.000034±0.000004	0.000003±0.000002	0.001	0.967	0.002	0.002
Firmicutes bacterium (no genus in NCBI)	0.02641±0.00319	0.02267±0.00168	0.01215±0.00157	0.001	0.466	0.008	0.001
Flintibacter	0.03154±0.00215	0.03061±0.00118	0.04347±0.00437	0.013	0.974	0.019	0.037
Fournierella	0.000006±0.000002	0.000012±0.000006	0.000077±0.00003	0.034	0.973	0.065	0.054
Fumia	0.000004±0.000004	ND	0.00003±0.00001	0.009	0.926	0.012	0.032
Gemella	0.01002±0.00246	0.0163±0.00345	0.00574±0.00123	0.03	0.241	0.025	0.496
Gilliamella	0.0003±0.00006	0.00019±0.00003	0.00008±0.00001	0.002	0.093	0.109	0.002
Gordonibacter	ND	ND	0.00005±0.00001	<0.001	>0.999	<0.001	<0.001
Hydrogenoanaerobacterium	0.000016±0.000005	0.000019±0.000006	0.000001±0.000001	0.038	0.887	0.041	0.12
Intestinimonas	0.00335±0.00033	0.00231±0.00041	0.00087±0.00039	0.002	0.183	0.042	0.001
Klebsiella	0.00011±0.00004	0.00026±0.0001	0.00001±0.00001	0.048	0.298	0.039	0.55
Lachnotalea	0.00059±0.00009	0.00035±0.00009	0.00014±0.00008	0.01	0.157	0.232	0.008
Lacrimispora	0.00056±0.00015	0.0003±0.00009	0.00008±0.00001	0.01	0.156	0.224	0.007
Lawsonibacter	0.78326±0.07654	0.97854±0.05095	0.42779±0.04105	<0.001	0.07	<0.001	0.002
Luxibacter	0.00005±0.00002	0.00007±0.00002	ND	0.024	0.727	0.022	0.118
Massiliimalia	0.00054±0.00015	0.00157±0.00017	0.00003±0.00001	<0.001	<0.001	<0.001	0.036
Merdimonas	0.00013±0.00004	ND	ND	0.001	0.002	>0.999	0.002
Mucispirillum	2.85145±0.64813	2.14127±0.33663	0.11829±0.10257	0.001	0.439	0.006	0.001
Muribaculaceae bacterium (no genus in NCBI)	1.37731±0.13964	0.94549±0.12529	1.3194±0.08399	0.039	0.054	0.083	0.937
Muribaculum	0.02347±0.00131	0.03872±0.00504	0.03374±0.00267	0.031	0.026	0.579	0.149
Natranaerovirga	0.00035±0.00006	0.00079±0.00019	0.00176±0.00039	0.007	0.499	0.049	0.007
Odoribacter	0.00016±0.00006	0.00018±0.00005	0.00104±0.00013	<0.001	0.978	<0.001	<0.001
Oscillibacter	0.98108±0.11104	1.22251±0.09204	1.89004±0.20204	0.002	0.509	0.014	0.002
Oscillospiraceae bacterium (no genus in NCBI)	2.00453±0.15707	2.20848±0.05381	1.60653±0.09879	0.003	0.393	0.003	0.049
Otoolea	0.00683±0.00057	0.00741±0.00048	0.0905±0.03182	0.012	>0.999	0.021	0.026
Parabacteroides	0.39545±0.05226	0.45501±0.07056	4.58344±0.39701	<0.001	0.985	<0.001	<0.001
Paramuribaculum	0.00126±0.00019	0.00189±0.00036	0.01578±0.00128	<0.001	0.855	<0.001	<0.001
Parasporobacterium	0.001028±0.000143	0.0015±0.000252	0.000007±0.000003	<0.001	0.171	<0.001	0.003
Parasutterella	0.00141±0.00015	0.00192±0.00026	0.231±0.04411	<0.001	>0.999	<0.001	<0.001
Peptococcaceae bacterium (no genus in NCBI)	0.30895±0.0277	0.32574±0.02324	0.2053±0.03047	0.014	0.906	0.016	0.049
Phocaeicola	0.85374±0.05582	0.62726±0.18032	0.04945±0.02432	0.001	0.386	0.007	0.001
Porphyromonadaceae bacterium (no genus in NCBI)	0.00175±0.00024	0.00284±0.00044	0.02945±0.00242	<0.001	0.873	<0.001	<0.001
Prevotella	3.23199±0.641	1.60038±0.41082	3.26332±0.34126	0.033	0.067	0.049	0.999
Provencibacterium	0.00201±0.00034	0.00127±0.00015	0.00064±0.00018	0.003	0.087	0.141	0.002
Pseudoflavonifractor	0.02489±0.00196	0.02605±0.00069	0.01115±0.00133	<0.001	0.824	<0.001	<0.001
Raoultibacter	0.000004±0.000003	0.000004±0.000004	0.000069±0.000008	<0.001	0.995	<0.001	<0.001
Robinsoniella	0.000001±0.000001	ND	0.000063±0.000017	0.001	0.995	0.002	0.004
Romboutsia	0.01419±0.00459	0.00074±0.00027	0.00011±0.00002	0.001	0.003	0.979	0.002
Roseburia	0.04084±0.00718	0.02202±0.00339	0.00351±0.00041	<0.001	0.019	0.016	<0.001
Ruminiclostridium	0.15258±0.0119	0.14365±0.00988	0.06813±0.00577	<0.001	0.784	<0.001	<0.001
Ruminococcus	0.01133±0.0003	0.01431±0.00203	0.05066±0.00673	<0.001	0.882	<0.001	<0.001
Sellimonas	0.00005±0.00001	0.00009±0.00002	0.00027±0.00006	0.005	0.774	0.018	0.006
Sodaliphilus	0.001±0.00026	0.00309±0.00041	0.01984±0.00198	<0.001	0.497	<0.001	<0.001
Sporofaciens	0.00936±0.0006	0.01869±0.00163	0.00817±0.00147	<0.001	0.001	<0.001	0.823
Staphylococcus	0.00005±0.00001	0.00003±0.00001	0.00242±0.00035	<0.001	0.998	<0.001	<0.001
Streptococcus	0.00346±0.00032	0.00359±0.00066	0.00098±0.0002	0.001	0.981	0.002	0.005
Subdoligranulum	0.00037±0.00005	0.00014±0.00003	0.00013±0.00004	0.003	0.007	0.987	0.005
Unclassified *Actinobacteria*	0.00046±0.00004	0.00051±0.00003	0.09412±0.03993	0.023	>0.999	0.037	0.047
Unclassified *Actinomycetia*	0.00105±0.00009	0.00099±0.00004	0.00042±0.00005	<0.001	0.791	<0.001	<0.001
Unclassified *Alphaproteobacteria*	0.00879±0.00399	0.00009±0.00004	0.00004±0.00001	0.014	0.024	>0.999	0.023
Unclassified *Atopobiaceae*	0.000001±0.000001	ND	0.000067±0.000014	<0.001	0.994	<0.001	<0.001
Unclassified *Bacillaceae*	0.0004±0.0001	0.00056±0.00007	0.00027±0.00004	0.03	0.298	0.023	0.403
Unclassified *Bacillales*	0.00011±0.00002	0.0002±0.00002	0.00008±0.00002	0.001	0.018	0.001	0.478
Unclassified *Bacteroidaceae*	7.30373±0.21834	5.17476±0.96659	0.36864±0.14026	<0.001	0.072	<0.001	<0.001
Unclassified *Bacteroidetes*	0.10775±0.01291	0.11795±0.01334	0.03107±0.00228	<0.001	0.784	<0.001	<0.001
Unclassified *Betaproteobacteria*	ND	ND	0.00005±0.00002	0.029	>0.999	0.046	0.058
Unclassified *Brachyspiraceae*	0.00007±0.00001	0.00003±0.00001	ND	<0.001	0.013	0.026	<0.001
Unclassified *Burkholderiales*	0.00008±0.00003	0.00005±0.00001	0.00244±0.00046	<0.001	0.996	<0.001	<0.001
Unclassified *Campylobacteraceae*	0.000131±0.00005	ND	0.000003±0.000002	0.005	0.008	0.995	0.009
Unclassified *Candidatus Saccharibacteria*	0.01435±0.00439	0.00015±0.00005	0.0064±0.00249	0.009	0.007	0.241	0.136
Unclassified *Candidatus Sumerlaeota*	0.00001±0.00001	0.00003±0.00001	ND	0.008	0.144	0.006	0.307
Unclassified *Clostridia*	0.81895±0.03998	0.62294±0.02742	0.49722±0.01846	<0.001	0.001	0.016	<0.001
Unclassified *Clostridiaceae*	0.05113±0.00969	0.05131±0.00485	0.02435±0.00339	0.009	>0.999	0.016	0.022
Unclassified *Coriobacteriales*	ND	0.000001±0.000001	0.00005±0.000016	0.004	0.997	0.008	0.009
Unclassified *Coriobacteriia*	0.00071±0.00019	0.00053±0.00006	0.00442±0.00063	<0.001	0.948	<0.001	<0.001
Unclassified *Desulfovibrionaceae*	0.27295±0.02209	0.26309±0.02165	0.13265±0.0117	<0.001	0.93	<0.001	<0.001
Unclassified *Eggerthellaceae*	0.01418±0.00231	0.01043±0.00068	0.15153±0.02011	<0.001	0.976	<0.001	<0.001
Unclassified *Eggerthellales*	0.00008±0.00001	0.00006±0.00001	0.00049±0.00009	<0.001	0.978	<0.001	<0.001
Unclassified *Enterobacterales*	0.000859±0.000116	0.000594±0.000305	0.000003±0.000002	0.024	0.627	0.108	0.023
Unclassified *Erysipelotrichaceae*	0.006±0.00036	0.00858±0.00156	0.01479±0.00324	0.039	0.705	0.14	0.039
Unclassified *Eubacteriales*	8.53653±0.85154	10.59975±0.54184	7.38941±0.46826	0.006	0.084	0.005	0.42
Unclassified *Muribaculaceae*	0.44521±0.04164	0.42073±0.05555	0.90811±0.07894	<0.001	0.961	<0.001	<0.001
Unclassified *Oceanospirillales*	ND	ND	0.00004±0.00001	<0.001	>0.999	<0.001	<0.001
Unclassified *Odoribacteraceae*	0.08445±0.0092	0.08179±0.01703	0.02821±0.0071	0.008	0.988	0.017	0.017
Unclassified *Paludibacteraceae*	0.0001±0.00001	0.00005±0.00001	ND	<0.001	0.012	0.007	<0.001
Unclassified *Pasteurellales*	0.00005±0.00002	0.00001±0.00001	ND	0.03	0.075	0.888	0.033
Unclassified *Peptococcaceae*	0.0009±0.00008	0.00123±0.0001	0.00068±0.00013	0.01	0.137	0.007	0.368
Unclassified *Peptostreptococcaceae*	0.00164±0.00056	0.00016±0.00004	0.00001±0.00001	0.002	0.007	0.923	0.003
Unclassified *Porphyromonadaceae*	ND	0.000243±0.000049	0.000004±0.000003	<0.001	<0.001	<0.001	0.996
Unclassified *Prevotellaceae*	0.00014±0.00003	0.00036±0.00006	0.00019±0.00006	0.038	0.044	0.105	0.83
Unclassified *Proteobacteria*	0.03902±0.00157	0.04053±0.00319	0.0278±0.00469	0.044	0.954	0.052	0.11
Unclassified *Pumilibacteraceae*	0.00027±0.00004	0.00029±0.00008	0.00001±0.00001	0.004	0.964	0.006	0.013
Unclassified *Selenomonadales*	ND	0.000073±0.000035	0.000001±0.000001	0.049	0.085	0.074	0.999
Unclassified *Spirochaetaceae*	0.00011±0.00004	0.00005±0.00001	0.00002±0.00001	0.037	0.162	0.611	0.031
Unclassified *Sporomusaceae*	0.00096±0.00011	0.00054±0.00017	0.00019±0.00011	0.005	0.113	0.177	0.004
Unclassified *Sutterellaceae*	0.0001±0.00002	0.00013±0.00001	0.00883±0.00161	<0.001	>0.999	<0.001	<0.001
Unclassified *Tannerellaceae*	0.00037±0.00004	0.00034±0.00003	0.0056±0.00099	<0.001	0.999	<0.001	<0.001
Unclassified *Veillonellales*	0.00005±0.00002	0.00002±0.00001	ND	0.004	0.053	0.305	0.003
Varibaculum	0.000012±0.000003	0.00001±0.000003	0.000162±0.000046	0.002	0.998	0.005	0.007
Vescimonas	0.000061±0.000033	0.000008±0.000003	ND	0.047	0.099	0.932	0.053

Table S4. Cecal organic acids

Organic acid (mmol /kg feces)	Sham	Control	PHGG	One-way ANOVA p-value	Tukey HSD p-value Sham vs Control	Control vs PHGG	Sham vs PHGG
Succinate	1.23±0.26	1.03±0.06	3.91±0.95	0.006	0.970	0.009	0.020
Lactate	ND	ND	33.07±33.07	0.427	>0.999	0.482	0.513
Formate	2.16±0.16	3.71±0.79	1.17±0.27	0.011	0.135	0.009	0.411
Acetate	43.27±1.63	44.11±4.62	46.16±9.88	0.953	0.996	0.973	0.953
Propionate	6.35±0.42	6.15±0.64	6.25±0.70	0.975	0.973	0.993	0.992
Butyrate	2.40±0.48	2.99±0.33	9.31±1.75	<0.001	0.928	0.003	0.002
Isobutyrate	1.10±0.06	1.48±0.16	0.66±0.13	0.001	0.133	<0.001	0.076
Valerate	0.25±0.14	0.004±0.004	0.02±0.02	0.047	0.061	0.987	0.080
Isovalerate	0.22±0.07	0.05±0.03	0.06±0.06	0.077	0.098	0.991	0.121

ND = Not detected

Table S5. Bacteria with α-glucosidase gene (%) that significantly different between groups at genus level

Genus	Sham	Control	PHGG	One-way ANOVA p-value	Tukey HSD p-value Sham vs Control	Control vs PHGG	Sham vs PHGG
Acutalibacter	0.00033±0.00009	0.00036±0.00004	0.00353±0.0005	<0.001	0.998	<0.001	<0.001
Alistipes	0.00035±0.00006	0.00021±0.00006	<0.00001	<0.001	0.113	0.016	<0.001
Anaerocaecibacter	0.00022±0.00004	0.00028±0.00008	0.00002±0.00001	0.007	0.690	0.007	0.046
Angelakisella	0.00052±0.00015	0.00031±0.00008	0.0001±0.00003	0.024	0.280	0.272	0.019
Bacteroidaceae bacterium (no genus in NCBI)	0.01625±0.0034	0.00782±0.00215	0.01592±0.00194	0.047	0.079	0.076	0.995
Bacteroides	0.0099±0.00097	0.00997±0.00237	0.01792±0.00259	0.032	>0.999	0.050	0.061
Bifidobacterium	0.00033±0.00008	0.0001±0.00001	0.01299±0.00524	0.018	0.999	0.029	0.041
Clostridiales bacterium (no genus in NCBI)	0.00003±0.00001	0.00003±0.00001	<0.00001	0.003	0.621	0.016	0.004
Clostridium	0.00017±0.00004	<0.00001	<0.00001	<0.001	0.000	0.995	<0.001
Dorea	0.00657±0.00037	0.00686±0.00105	0.00289±0.00032	0.002	0.957	0.003	0.007
Eubacterium	0.00016±0.00009	0.00186±0.00048	0.00424±0.00082	0.001	0.147	0.026	0.001
Faecalibaculum	0.00034±0.00007	0.00023±0.00005	0.00149±0.00039	0.004	0.948	0.006	0.016
Flavonifractor	0.00011±0.00001	0.00006±0.00002	0.00005±0.00001	0.024	0.087	0.740	0.023
Lawsonibacter	0.00085±0.00012	0.001±0.00008	0.00044±0.00005	0.001	0.418	0.001	0.014
Muribaculaceae bacterium (no genus in NCBI)	0.00216±0.00038	0.00119±0.00022	0.00202±0.00015	0.032	0.043	0.072	0.918
Oscillibacter	0.00108±0.00014	0.00123±0.00015	0.00305±0.00037	<0.001	0.905	<0.001	<0.001
Oscillospiraceae bacterium (no genus in NCBI)	0.00307±0.00032	0.00352±0.00014	0.00185±0.00019	<0.001	0.342	<0.001	0.004
Otoolea	<0.00001	<0.00001	0.00012±0.00004	0.004	>0.999	0.007	0.010
Parabacteroides	0.0005±0.00009	0.00061±0.00004	0.00836±0.00124	<0.001	0.995	<0.001	<0.001
Phocaeicola	0.01054±0.00033	0.00708±0.00155	0.00048±0.00028	<0.001	0.069	0.001	<0.001
Prevotella	0.00361±0.00069	0.00186±0.00049	0.00384±0.00036	0.028	0.077	0.034	0.950
Roseburia	0.00005±0.00002	0.00002±0.00001	<0.00001	0.033	0.339	0.289	0.026
Ruminococcus	0.00001±0	0.00003±0.00001	0.00017±0.00004	0.002	0.886	0.007	0.004
Unclassified *Bacteroidaceae*	0.01452±0.00046	0.00985±0.00175	0.0005±0.00024	<0.001	0.029	<0.001	<0.001
Unclassified Bacteroidales	0.01004±0.0016	0.0103±0.00164	0.00261±0.00026	0.001	0.989	0.002	0.004
Unclassified Bacteroidia	0.00006±0	0.00003±0.00001	0.00023±0.00006	0.003	0.877	0.004	0.015
Unclassified Clostridia	0.00121±0.00016	<0.00001	<0.00001	<0.001	<0.001	0.999	<0.001
Unclassified *Clostridiaceae*	0.00018±0.00006	0.00034±0.00005	0.00014±0.00003	0.021	0.090	0.021	0.806
Unclassified Eubacteriales	0.00441±0.00046	0.0058±0.0008	0.00985±0.00162	0.012	0.681	0.052	0.013
Unclassified Firmicutes	0.00007±0.00001	0.00009±0.00002	0.00354±0.00158	0.035	>0.999	0.054	0.065
Unclassified *Muribaculaceae*	0.00024±0.00004	0.00021±0.00004	0.0007±0.00018	0.012	0.980	0.017	0.033
Unclassified *Oscillospiraceae*	0.00038±0.00011	0.00032±0.0001	0.00003±0.00001	0.023	0.873	0.061	0.030

Table S6. Bacteria with mannan endo-β-1,4-mannosidase gene (%) that significantly different between groups at genus level

Genus	Sham	Control	PHGG	One-way ANOVA p-value	Tukey HSD p-value Sham vs Control	Control vs PHGG	Sham vs PHGG
Acutalibacter	0.00002±0.00001	0.0001±0.00003	0.00111±0.00036	0.006	0.971	0.013	0.012
Alistipes	0.00051±0.00014	<0.00001	<0.00001	<0.001	<0.001	>0.999	<0.001
Lachnospiraceae bacterium (no genus in NCBI)	0.00156±0.00019	0.00245±0.00055	0.04186±0.01058	0.001	0.995	0.002	0.002
Oscillospiraceae bacterium (no genus in NCBI)	0.00060±0.00009	0.00079±0.00006	0.00006±0.00005	<0.001	0.158	<0.001	<0.001
Prevotella	0.00251±0.00047	0.00123±0.00033	0.00264±0.00032	0.027	0.071	0.035	0.964
Unclassified Bacteria	0.00174±0.00036	0.00173±0.00035	0.00007±0.00005	0.001	>0.999	0.002	0.003
Unclassified *Bacteroidaceae*	0.00131±0.00018	0.00111±0.00043	0.00011±0.00007	0.019	0.870	0.053	0.026
Unclassified Bacteroidales	0.00717±0.00104	0.00708±0.00116	0.00202±0.0003	0.001	0.997	0.003	0.004
Unclassified Bacteroidia	0.00005±0.00001	0.00004±0.00001	0.00037±0.00003	<0.001	0.945	<0.001	<0.001
Unclassified Ktedonobacterales	0.00071±0.00010	0.00094±0.00014	<0.00001	<0.001	0.297	<0.001	0.001
Unclassified *Lachnospiraceae*	0.00540±0.00062	0.00369±0.00202	0.00003±0.00001	0.030	0.633	0.130	0.029
Unclassified *Muribaculaceae*	0.00017±0.00003	0.00013±0.00001	0.00059±0.00014	0.004	0.951	0.006	0.016
Unclassified *Rikenellaceae*	0.00029±0.00007	<0.00001	<0.00001	<0.001	<0.001	>0.999	<0.001

Table S7. Enriched KEGG pathways in microbiome of PHGG group.

KEGG ID	Description	Gene Ratio	Rich Factor	Fold Enrichment	q-Value	Count	GeneID
Upregulated pathway in PHGG group compared to the control							
map00051	Fructose and mannose metabolism	10/348	0.089	3.485	0.010	10	K00966/K00011/K02798/K01218/K22252/K19956/K02771/K01623/K00844/K00045
map00061	Fatty acid biosynthesis	5/348	0.128	5.004	0.027	5	K00668/K11263/K18474/K11533/K00209
map00400	Phenylalanine, tyrosine and tryptophan biosynthesis	7/348	0.095	3.692	0.027	7	K01713/K04093/K00832/K18240/K00815/K04092/K13829
map00500	Starch and sucrose metabolism	10/348	0.094	3.682	0.007	10	K05988/K01179/K06896/K06859/K00690/K05343/K20108/K00844/K16147/K00692
map00520	Amino sugar and nucleotide sugar metabolism	15/348	0.096	3.753	0.001	15	K01654/K00966/K13015/K02472/K07102/K01097/K22252/K06859/K01452/K10046/K00844/K01233/K15896/K08068/K00886
map00541	O-Antigen nucleotide sugar biosynthesis	8/348	0.081	3.154	0.032	8	K01654/K13015/K19180/K02472/K22252/K16704/K15896/K08068
map00550	Peptidoglycan biosynthesis	6/348	0.113	4.419	0.025	6	K21465/K08724/K11695/K05363/K21464/K12554
map00620	Pyruvate metabolism	12/348	0.090	3.522	0.004	12	K18118/K01512/K01596/K22211/K04073/K00156/K12972/K11263/K18930/K00245/K07248/K01595
map00640	Propanoate metabolism	8/348	0.082	3.219	0.029	8	K00048/K01903/K01720/K01902/K01692/K11263/K13921/K01965
map00680	Methane metabolism	16/348	0.082	3.203	0.002	16	K01070/K05884/K12234/K11212/K08093/K03532/K22015/K01623/K03533/K05979/K14940/K07812/K01595/K19793/K14083/K18933
map00920	Sulfur metabolism	11/348	0.101	3.939	0.003	11	K00955/K00390/K01082/K08358/K17994/K17218/K21308/K16937/K07308/K16936/K08357
map00930	Caprolactam degradation	4/348	0.182	7.097	0.025	4	K01692/K01053/K06446/K01453
map01054	Nonribosomal peptide structures	6/348	0.118	4.592	0.025	6	K15664/K15668/K16095/K15654/K15662/K16129
map01200	Carbon metabolism	19/348	0.052	2.032	0.027	19	K00030/K18118/K00616/K01070/K01903/K06859/K01902/K11263/K08093/K01053/K22015/K01623/K00844/K00245/K01965/K01595/K14083/K00886/K00209
map01240	Biosynthesis of cofactors	26/348	0.069	2.706	<0.001	26	K00966/K05936/K02496/K01432/K01919/K05884/K12234/K20862/K11212/K02302/K18240/K13950/K01053/K02858/K21479/K03635/K03146/K10046/K01113/K03638/K05979/K09882/K19793/K14153/K01440/K18933
map01250	Biosynthesis of nucleotide sugars	17/348	0.081	3.145	0.001	17	K01654/K00966/K19180/K07031/K02472/K07102/K15669/K01097/K22252/K16704/K13307/K10046/K00844/K15896/K08068/K00886/K13311
map01503	Cationic antimicrobial peptide (CAMP) resistance	6/348	0.111	4.337	0.026	6	K01364/K07771/K03673/K14205/K13632/K18073
map02020	Two-component system	46/348	0.092	3.598	<0.001	46	K07677/K08082/K01179/K07690/K02472/K07670/K09474/K07675/K11615/K07771/K03620/K07653/K02668/K07647/K11712/K20264/K08358/K07717/K07663/K11711/K20489/K19661/K03532/K19616/K10125/K07770/K14205/K07686/K13532/K00245/K01113/K03533/K08372/K10909/K11356/K18073/K00371/K18351/K07673/K08357/K00370/K11622/K13040/K14987/K00990/K00692
map02024	Quorum sensing	18/348	0.064	2.483	0.007	18	K10557/K11530/K01364/K10556/K10555/K20276/K10558/K06998/K01218/K08321/K20264/K03071/K11216/K20333/K20489/K10909/K15654/K15852
map02025	Biofilm formation - Pseudomonas aeruginosa	8/348	0.089	3.470	0.025	8	K11912/K03651/K20971/K21022/K20997/K21019/K20968/K21005
map02060	Phosphotransferase system (PTS)	9/348	0.125	4.879	0.003	9	K02806/K02798/K02771/K20108/K02773/K02774/K02821/K11183/K02784
map04122	Sulfur relay system	5/348	0.172	6.730	0.012	5	K03636/K03635/K03638/K11996/K21140
Downregulated pathway in PHGG group compared to the control							
map00052	Galactose metabolism	12/432	0.154	4.838	<0.001	12	K02082/K21621/K02747/K02746/K12111/K02745/K01631/K16370/K00917/K07406/K08302/K15778
map00130	Ubiquinone and other terpenoid-quinone biosynthesis	11/432	0.186	5.863	<0.001	11	K05928/K18285/K11783/K11782/K11785/K11784/K03182/K03186/K20810/K00355/K00568
map00520	Amino sugar and nucleotide sugar metabolism	21/432	0.135	4.233	<0.001	21	K12453/K12409/K12454/K10011/K15895/K15898/K15855/K15856/K15894/K13016/K15897/K00621/K10012/K09001/K02473/K16881/K00884/K08679/K06118/K15913/K15778
map00541	O-Antigen nucleotide sugar biosynthesis	11/432	0.111	3.494	0.005	11	K12453/K12454/K15895/K15898/K21379/K15856/K15894/K13016/K15897/K02473/K08679
map00564	Glycerophospholipid metabolism	11/432	0.096	3.008	0.017	11	K01114/K06132/K00894/K00113/K03735/K05929/K00112/K03736/K04019/K17830/K00111
map00920	Sulfur metabolism	16/432	0.147	4.616	<0.001	16	K17229/K15552/K17725/K17230/K02047/K02045/K02048/K15551/K02046/K10831/K00958/K07306/K00395/K11181/K11180/K00394
map01240	Biosynthesis of cofactors	29/432	0.077	2.432	<0.001	29	K05928/K15734/K03795/K18285/K11783/K11782/K11785/K10977/K08310/K11784/K03182/K03186/K03153/K04032/K02170/K20810/K01906/K02191/K00002/K20967/K00128/K01772/K00355/K13541/K21063/K08679/K03148/K22225/K00568
map01250	Biosynthesis of nucleotide sugars	22/432	0.104	3.279	<0.001	22	K12453/K12409/K12454/K10011/K15895/K16436/K15898/K21379/K15856/K12710/K15894/K13016/K15897/K00621/K09001/K02473/K00884/K08679/K06118/K15913/K13308/K15778
map02024	Quorum sensing	19/432	0.067	2.111	0.025	19	K01114/K20374/K01318/K15656/K13815/K20531/K20485/K20484/K07813/K20483/K14645/K07715/K02490/K20345/K20344/K10917/K20342/K20266/K20533
map02025	Biofilm formation - Pseudomonas aeruginosa	13/432	0.144	4.542	<0.001	13	K11901/K11893/K11891/K11900/K11903/K11895/K21020/K06596/K21012/K02658/K20973/K10941/K11444
map02020	Two-component system	52/432	0.104	3.277	<0.001	52	K07639/K03776/K07661/K00404/K07701/K15012/K11633/K11521/K07700/K02106/K13815/K07659/K07785/K20485/K06596/K18866/K18444/K07783/K07792/K07654/K02658/K01034/K20484/K01035/K18348/K18941/K11629/K07644/K13599/K13598/K07813/K20483/K11329/K18856/K13533/K07777/K20973/K10941/K13587/K10943/K10682/K07664/K07715/K02490/K11616/K07638/K05966/K11630/K11444/K02406/K07665/K07669
map02040	Flagellar assembly	7/432	0.127	4.002	0.025	7	K02393/K10941/K02424/K02394/K10943/K02386/K02406
map03070	Bacterial secretion system	11/432	0.149	4.674	<0.001	11	K02460/K02452/K11906/K11891/K11903/K11892/K02454/K03117/K03194/K03072/K02455
map04122	Sulfur relay system	5/432	0.172	5.421	0.026	5	K21028/K07236/K03148/K11179/K07235
map05111	Biofilm formation - Vibrio cholerae	12/432	0.113	3.560	0.003	12	K20959/K02460/K02452/K20956/K20965/K20962/K03087/K02454/K10941/K10943/K10917/K02455